

## HEAT TRANSFER PROCESSES IN A TURBULENT FLOW ALONG REGULAR RELIEFS OF SPHERICAL CONCAVITIES

V. N. Afanas'ev, P. S. Roganov, and Ya. P. Chudnovskii

UDC 536.24

*The experimental study of friction and heat exchange in a flow along surfaces with a systems of spherical recesses of various densities are presented.*

Recently, the attention of researchers has been drawn to studies [1, 2], which suggest using ordered systems of spherical recesses as heat transfer enhancers. For a flow of a heat transfer agent along such reliefs, the authors [1] discovered and studied, in general outline, self-developing dynamic vortex structures, flowing out of the recesses in the form of jets and providing a high-rate mass transfer from a surface to a core of the main flow. Precisely the high-rate mass transfer of the heat transfer agent from a near-wall region of the flow to its outer part is the primary cause of a decrease in thermal resistance at the surface transferring heat and, hence, of a heat transfer enhancement. Moreover, the authors [2] point out that a flow along such reliefs is not associated with an increase in surface friction.

The new type of self-developing flow above a three-dimensional spherical recess, revealed in [1], has not been diagnosed sufficiently until now, which, undoubtedly, hinders both its theoretical description and the creation of simple engineering techniques for calculating the friction and heat exchange at the like surfaces. Therefore, to substantially extend a set of experimental data on a flow along such reliefs, the authors of the present study performed investigations into the friction and heat exchange at the surfaces, profiled by the systems of spherical recesses, with an external nongradient air flow passing along them at Reynolds numbers ranging from 500 to 2500 across the momentum thickness. The experiments were conducted on a test bed specially manufactured for diagnostics of a boundary layer.

A basic unit of the test bed is a subsonic free-jet wind tunnel operating on the principle of suction. A working section of the wind tunnel is a  $0.08 \times 0.3 \times 1.1$  m flow channel, on whose lower detachable wall the considered boundary layer develops. Besides, a heating panel is located on the lower wall of the working section, which permits a heating of the studied specimen by the law  $q = \text{const}$ . A flow convergence due to the growth of the boundary layer was compensated for by a small apex angle of the flow channel.

The structure of the wind tunnel enables us to obtain a velocity profile that is practically uniform (with nonuniformity smaller than 5%) at the entrance to the working section, which forms a low-turbulent isotropic flow, whereas the employed ventilator provides a velocity variation in the main flow velocity from 2 up to 20 m/sec.

Study [3] reports a detailed description of the test bed and of the experimental technique.

As test specimens, we used nine plates with the systems of spherical recesses, whose geometrical parameters are shown in Fig. 1 and given in Table 1. Geometric parameters of the profiling were chosen such that a nonseparating flow along the relief under consideration was ensured.

In the current study, the working specimens were produced via grinding steel plates and subsequently milling the system of spherical recesses of specified geometry on numerical-controlled horizontal milling machines to a tolerance not larger than  $\pm 0.02$  mm. The working reliefs were given a uniform light coating of lacquer (of NTs 201 type) to rule out the possibility of electric contact between the measuring probe and the surface of the working sample.

In the experimental investigation, a mean velocity, a temperature, and their fluctuations were measured with the aid of a 55M hot-wire anemometric set fabricated by the DISA Electronics Company. The boundary layer was diagnosed through standard unifilar probes with a sensitive element  $2.5 \mu\text{m}$  in diameter. During the measurement, the probe was arranged on (above) an initially smooth region of the profiled specimen surface.

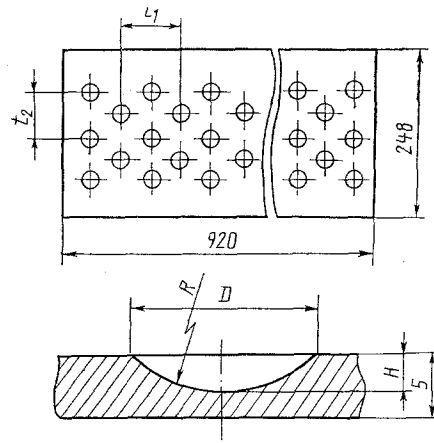


Fig. 1. Geometric parameters of test specimens.

TABLE 1. Geometric Parameters of Working Surfaces

No.	$D$ , mm	$H$ , mm	$R$ , mm	$t_1$ , mm	$t_2$ , mm	$f$ , %	Designation (see Figs. 2-4)
1	7,5	0,5	13,32	13,3	11,5	25	1
2	6,0	0,4	10,20	10,6	9,1	25	
3	4,5	0,3	7,65	8,0	7,5	25	
4	7,5	0,5	13,32	9,4	8,1	50	2
5	6,0	0,4	10,20	7,5	6,5	50	
6	4,5	0,3	7,65	5,6	4,9	50	
7	7,5	0,5	13,32	8,4	7,3	70	3
8	6,0	0,4	10,20	6,4	5,5	70	
9	4,5	0,3	7,65	4,8	4,2	70	

Local friction coefficients were determined, using the known Clauser method [4], from a logarithmic range of the velocity profile, and a local density of the heat flux was obtained with the help of heat flux probes DTP-0.5 designed and manufactured in the Thermometry Department of the Institute of Engineering Thermophysics, Academy of Sciences of the Ukrainian SSR. Thermal resistance of these probes comprises about  $0.001 \text{ K} \cdot \text{m}^2/\text{W}$ , which does not introduce any appreciable distortions in a temperature field of the considered working specimen.

The performed analysis of possible measurement errors allowed a determination of maximal mean-square errors of the measured quantities, which are in a good agreement with the errors, generally accepted for diagnostics of boundary layers under similar operating conditions. Furthermore, results of the tests, carried out on the smooth specimen, are well consistent with data [5, 6].

The hydrodynamics of a flow in a turbulent boundary layer can be judged from a velocity distribution, while the heat transfer can be estimated from temperature profiles. A combined measurement of the velocity and temperature distributions in a liquid or gas flow enables a quantitative analysis and comparison of the heat exchange in various regions of the boundary layer, including a viscous sublayer. To this end, the authors executed thorough measurements for the velocity and temperature profiles near the wall. Such measurements give grounds for a quantitative analysis.

Analyzing the obtained experimental data demonstrated a virtually identical variation in the characteristics of the boundary layer in question for all specimens with the same density of the surface profiling. In this connection, the plots will compare only between relevant data for the specimens with different densities of recesses on the fairing.

It is well known that an effective enhancement of the heat transfer from a rough wall to a flow is possible when a drag of the viscous sublayer decreases owing to generation, by roughness elements, of a vortex flow in the near-wall region. However, as is indicated in [7], in this case a rise in the water drag must occur, which is determined by a form drag for individual roughness elements.

Figure 2 gives velocity and temperature distributions in the turbulent boundary layer on profiled specimens.

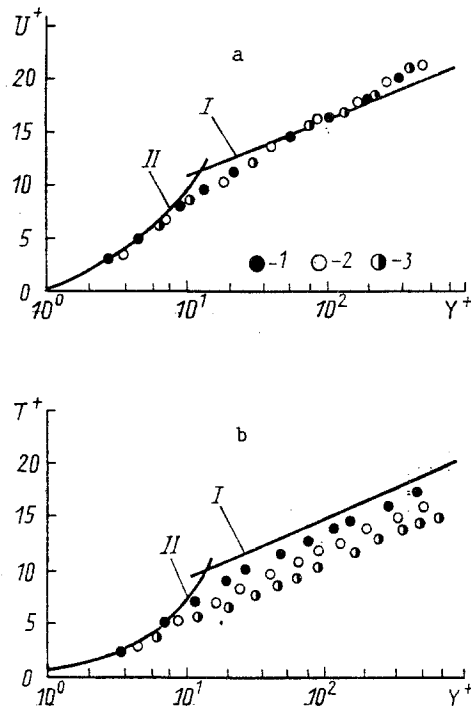


Fig. 2. Distribution of mean velocities (a) and temperatures (b) in a turbulent boundary layer on profiled surfaces: a) I,  $U = 5.6 \log Y^+ + 4.9$ ; II,  $U^+ = Y^+$ ; b) I,  $T^+ = 5.9 \log Y^+ + 3.2$ ; II,  $T^+ = Pr Y^+$ .

A good agreement between the compared data and the universal logarithmic law for a smooth wall is evident from the analysis presented in Fig. 2a, which allows a conclusion that such (nonseparation) profiling of the surface does not exert any noticeable effect on the flow hydrodynamics.

As for the mean temperature distribution over the thickness of the considered boundary layer, it ensues from Fig. 2b that stratification of the obtained temperature profiles is observed in logarithmic coordinates, depending on the profiling density of the working specimen surface. In this case, the greater the density of recesses on the fairing, the larger the deviation of the temperature profile from the universal logarithmic law towards a heat transfer enhancement.

Analyzing fluctuation distributions for the profiled specimens (Fig. 3) points to a certain tendency to a shift of the fluctuation maxima towards the fairing, which indicates a decrease in the thickness of the viscous sublayer on the profiled specimens as compared to the smooth surface and, as a consequence, a reduction in the thermal resistance to the heat transfer.

Figure 4 presents experimental values of the local Stanton numbers in comparison with a familiar heat exchange law for a smooth surface (I):  $St = 0.0144(Re_T^{**})^{-0.25}$ . Obviously, the obtained data exceed heat transfer coefficients characteristic of the smooth surface, with the Stanton numbers increasing in direct proportion to the profiling density of the working specimen.

The Stanton numbers, obtained in the experiments on profiled specimens, were generalized to an accuracy of 8-10% by the following relation

$$St = 0.0144 \left( 1 + \frac{f}{2} \right) \frac{F_0}{F_D} (Re_r^{**})^{-0.25},$$

suitable for engineering estimation of the heat transfer on such reliefs over the studied range of geometric parameters and operating conditions. Additionally, Fig. 4 gives experimental local coefficients of surface friction, whose values actually coincide, in the considered range of Reynolds numbers, with a "standard" friction law for a smooth wall (II):  $C_f = 0.0126(Re^{**})^{-0.25}$ .

Thus, the simultaneous analysis of the friction and heat transfer at the surfaces, profiled by spherical recesses, discloses a considerable enhancement (by up to 35-40%) of the heat transfer as against the smooth wall, with the water drag practically unchanged. Here the degree of the heat transfer enhancement grows as the profiling density of the fairing increases.

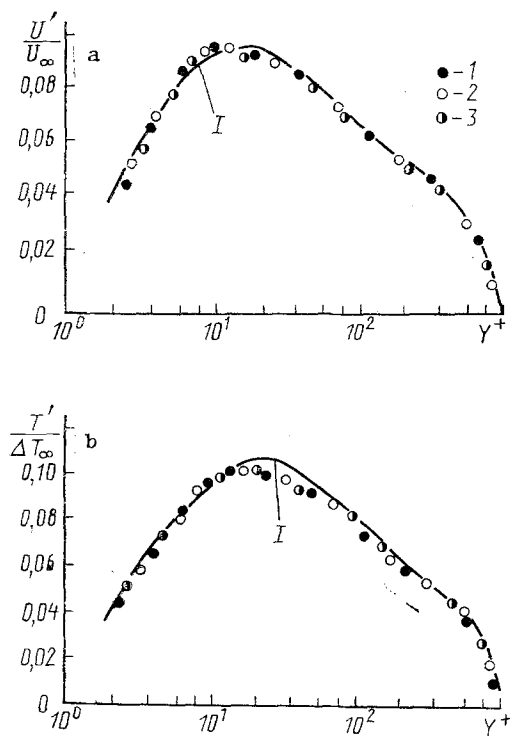


Fig. 3. Distributions of longitudinal components of velocity (a) and temperature (b) fluctuations at profiled surfaces: I) smooth specimen.

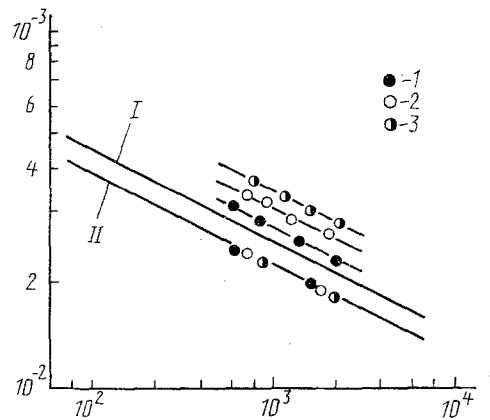


Fig. 4. Friction and heat transfer at the surfaces with the systems of spherical recesses: I)  $St = 0.0144 (Re_T^{**})^{-0.25}$ ; II)  $C_f = 0.0126 (Re_T^{**})^{-0.25}$ .

In our opinion, the results obtained in the given study and the achieved effect of the heat transfer enhancement may be attributable to a certain decrease in the thickness of the viscous sublayer by the action of the concavities, as well as to three-dimensionally of the recesses, which sets up a near-wall pressure gradient, mainly governing the heat transfer mechanism in this region.

#### NOTATION

$y$ , coordinate running normal to the fairing, m;  $u$ , running value of mean velocity, m/sec;  $u_\infty$ , mean velocity of the main flow, m/sec;  $\Delta T = T_w - T$ , mean temperature difference between the wall and the flow, K;  $U^+ = u/u_\infty$ , dimensionless velocity;  $T^+ = (\Delta T/\Delta T_\infty)(1/\sqrt{St})$ , dimensionless temperature;  $Y^+ = u_\tau y/\nu$ , dimensionless coordinate;  $f = \pi D^2/4t_1 t_2$ , density of the surface

profiling;  $F_0$ , area of the initially smooth surface,  $m^2$ ;  $F_p$ , area of the profiled surface,  $m^2$ ;  $C_p$ , local friction coefficient;  $St$ , Stanton number;  $Re^{**}$ ,  $Re_T^{**}$ , Reynolds numbers over the thickness of momentum and energy loss.

#### LITERATURE CITED

1. G. I. Kikhadze, Yu. K. Krasnov, A. M. Podymako, and V. B. Khabenskii, Dokl. Akad. Nauk SSSR, **291**, No. 6, 1315-1318 (1986).
2. I. A. Gachechiladze, G. I. Kiknadze, Yu. K. Krasnov, et al., Heat Transfer-MIF. Convective, Radiative and Combined Heat Transfer. Key-note papers [in Russian], Minsk (1988), pp. 83-125.
3. V. N. Afanas'ev, A. I. Leont'ev, and Ya. P. Chudnovskii, "Friction and heat transfer at the surfaces profiled by spherical recesses," Preprint Moscow State Technical University, No. 1-90, Moscow (1988).
4. F. Clauser, Problems of Mechanics, No. 2, 297-340 (1959).
5. P. S. Klebanoff and Z. W. Diehl, NASA Report, No. 1110 (1952).
6. E. V. Shishov, V. P. Yugov, V. N. Afanas'ev, et al., Tr. Mosk. Vyssh. Tekh. Uchil., No. 222, 121-129 (1976).
7. A. A. Zhukauskas, Convective Transfer in Heat Exchangers [in Russian], Moscow (1982).

### ANALOG OF THE RAYLEIGH EQUATION FOR THE PROBLEM OF BUBBLE DYNAMICS IN A TUBE

Yu. B. Zudin

UDC 536.248.2.001.5

*Analysis is made of the growth of a vapor (gas) bubble in a horizontal tube filled with an ideal liquid.*

As is well known [1], the dynamics of a gas (vapor) bubble in an unrestricted volume of an ideal liquid is described by the Rayleigh equation

$$\frac{\Delta P}{\rho} = \frac{P'' - P_\infty}{\rho} = \frac{3}{2} \dot{R}^2 + R\ddot{R}. \quad (1)$$

For the problem of bubble growth in a tube, vital for a number of applications connected with boiling, the "spherical" equation (1) is inapplicable in the general case. The present work gives the derivation of a "cylindrical" analog for the Rayleigh equation (1).

We consider first the case of expansion of a spherical bubble in the symmetry center of a horizontal tube with radius  $R_0$  and length  $2l$  (Fig. 1a). We obtain the pressure difference between the bubble  $P''(t)$  and the liquid at the outlet from the tube  $P_\infty = \text{const}$  by integrating the  $z$ -projection of a momentum equation for  $z$  at  $r = 0$  going from  $z = R$  (bubble surface) to  $z = l$  (outlet from the tube):

$$\frac{P'' - P_\infty}{\rho} = \frac{1}{2} (u_l^2 - u_R^2) + \int_R^l \frac{\partial u}{\partial t} dz. \quad (2)$$

To calculate the right side of Eq. (2) we consider the velocity field from a point mass source at the axis of an infinite tube [2]. The velocity potential  $\varphi$  and the longitudinal velocity  $u$  at the axis  $z$  (for  $r = 0$ ) of the flow are written in the form

$$\bar{\varphi} = \frac{\varphi}{u_\infty} = -\frac{1}{2z} - \frac{1}{\pi} \int_0^\infty \frac{K_1(\varepsilon)}{I_1(\varepsilon)} \cos(\varepsilon z) d\varepsilon, \quad (3)$$